Highly Active and Cheap Graphite/PTFE Composite Coating Cathodes for Electrogeneration of Hydrogen Peroxide

Kang Wang (1664102752@qq.com)
Nanjing Tech University
Zhaolian Zhu
Nanjing Tech University https://orcid.org/0000-0002-2700-4875
Dan Xu
Nanjing Tech University
Muyao Li
Nanjing Tech University
Shiyu Yuan
Nanjing Tech University
Hailing Wang
Nanjing Tech University

Research Article

Keywords: Hydrogen peroxide,Electrogeneration, Oxygen reduction reaction, Coating cathode, Current efficiency

Posted Date: February 2nd, 2022

DOI: https://doi.org/10.21203/rs.3.rs-991342/v1

Abstract

Using cheap graphite powder as catalyst and polytetrafluoroethylene (PTFE) as binder, graphite/PTFE composite coating cathodes were fabricated for efficient electrochemical synthesis of hydrogen peroxide (H_2O_2) in a no-diaphragm electrolysis system. A series of experiments were conducted to examine the influence of different factors, such as cathode thickness, cathode area, solution pH, and current density on H_2O_2 electrogeneration. Adjusting the thickness and area of the cathode was demonstrated to be effective in optimizing the electrocatalytic properties in oxygen reduction reaction (ORR). Among the cathodes investigated, the cathode with the thickness of 0.75 mm and area of 16 cm^2 achieved the highest H_2O_2 accumulation and current efficiency (CE). The H_2O_2 accumulation reached 207.5 $mg{\cdot}L^{-1}$ and CE reached 34.1% in 180 min when the current density is 5 $mA{\cdot}cm^{-2}$ and the initial pH is 3.0. The present work successfully develops a simple approach to enhance the H_2O_2 electrogeneration, as well as the corresponding CE, through optimization of cathode geometric parameters and operation conditions.

1 Introduction

$H_2O_2$is a valuable chemical and has a diverse range of practical applications,including pulp and textile bleaching (Hage et al. 2006), chemical synthesis(Zhang et al. 2020), wastewater and ballast water treatment(Kim et al. 2020; Liu et al. 2018),exhaust air treatment(Yang et al. 2018),semiconductor cleaning (Seh et al. 2017), as well as medical and cosmetic uses (Melchionna et al. 2019). The global H_2O_2market demand exceeded 3.85 million tons in 2015 and is projected to surpass 6.0 million tons by 2024 due to its wide and promising applications (Kim et al. 2018).

At present, the industrial synthesis of H_2O_2predominantlyrelies on the highenergy-consuming and waste-producing anthraquinone process, which involves continuous hydrogenation and oxidation of anthraquinone molecules in the presence of expensive palladium catalysts (Xia et al. 2019). Anthraquinone process is suitable for large-scale production of H_2O_2, and the concentration of H_2O_2 is usually about 30%. Furthermore, the easy decomposition and instability of high-concentration H_2O_2lead togreat safety risks for transportation,handlingand storage (Li et al. 2020). As a simple, easily operable and eco-friendly process,electrochemical synthesis of H_2O_2 by ORRstands out as a potential alternative route to anthraquinone process, which could permit in situ generation to minimize transportation and storage costs (AlJaberi et al. 2019; Wang et al. 2021).

ORR has two pathways: the two-electron (2 e^-) pathway where H_2O_2 is generated through partial reduction of O_2(Eq.1 and 2), and the four-electron (4e^-) pathway where oxygen (O_2) is completely reduced to water instead (Eq.3 and 4). Thus, to produce H_2O_2effectively, it is necessary to promote the2 e^- pathway andsuppressthe 4 e^- pathway.

2 e^- pathway:

(alkaline media)

$$O_2 + 2H_2O + 2e^- \rightarrow H_2O_2 + 2OH^- \quad (0.06\ V_{RHE}) \tag{1}$$

(acid media)

$$O_2 + 2H^+ + 2e^- \rightarrow H_2O_2 \quad (0.70\ V_{RHE}) \tag{2}$$

4 e^- pathway:

(alkaline media)

$$O_2 + 2H_2O + 4e^- \rightarrow 4OH^- \quad (0.40\ V_{RHE}) \tag{3}$$

(acid media)

$$O_2 + 4H^+ + 4e^- \rightarrow 2H_2O \quad (1.23\ V_{RHE}) \tag{4}$$

Various noble metals and their alloys have been suggested as prospective catalysts for H_2O_2 production (Jiang et al. 2018).For example, Pt-Hgwere highly active and selective for 2 e^- ORR, on which the H_2O_2 selectivity was already 96% at a potential in the range 0.2–0.4 V versus RHE (Siahrostami et al. 2013).Unfortunately, the high cost and sophisticated fabrication process of noble metal-based electrocatalysts will be major bottlenecks in their industrial and household applications. Thus, metal-free carbon-based materials are regarded as promising substitutes due to their global abundance, low price and apparent ORR activity (Moreira et al. 2019; Pham-Truong et al. 2018). Currently, various carbonaceous materialshave been successfully developed as catalyticmaterials for selective H_2O_2synthesis, including graphite (Da Pozzo et al. 2005), graphite felt (Wang et al. 2015; Zhao et al. 2020), reticulated glassy carbon foam (Zhou et al. 2018), carbon felt (Pérez et al. 2018; Ma et al. 2019), and activated carbon fiber (Wang et al. 2005). In a recent study(Xia et al. 2015), polyacrylonitrile-based carbon fiber brush (PAN-CF) was employed to promote the 2 e^- ORR. The H_2O_2 concentration reached 90.4 $mg{\cdot}L^{-1}$in 60 min, which may be attributed to catalytic selectivity of the nitrogen-doped structure in PAN-CF. Additionally, Zarei et al. (2009) found that theH_2O_2concentration obtained using carbon nanotube-PTFE electrode was almost 30 times as high as that of graphite felt electrode. The porous surface of the nanotube-PTFE electrode plays a key role in increasingoxygen transfer rates, thereby achieving enhanced mass transfer and high-efficiency H_2O_2production.

To further improve the catalytic activity and selectivity of carbon-basedcatalystsfor 2e^- ORR, many modification methods have been utilizedto optimize their porous structures,surface functional groupsand surface area (Park et al. 2014; Thostenson et al. 2017; Shiraishi et al. 2015). For instance,Zhou et al. (2013) claimed that the modified graphite felt electrode displayed higher electrocatalytic activity for 2 e^- ORR. The H_2O_2 concentration reached 247.2 $mg{\cdot}L^{-1}$, which was 2.6 times that of the unmodified

electrode.Liu et al. (2015) found that the hierarchically porous carbon (HPC) maintained high H_2O_2 selectivity (80.9–95.0%) under acidic conditions, which was comparable to those of noble metal-based ORR electrocatalysts. They also demonstrated that the goodcatalytic activity and selectivity of HPC toward H_2O_2 were related to the high extent of sp^3-C bonds and defects formed during hydrothermal treatment and carbonization process under H_2.

Besides catalyst microstructures, electrode macro design parameters play critical roles in mass transfer and energy efficiency in different types of electrochemical systems(Oliaii et al. 2018). Nevertheless, little is known on the influence of cathode thickness and area on H_2O_2 electrosynthesis efficiency via ORR. In the present study, a series of cathodes were prepared by a simple coating method with stainless steel mesh as matrix, graphite powder as catalyst and polytetrafluoroethylene as binder, and the effects of electrode thickness, area and electrochemical process parameters on H_2O_2 yield and CE were systematically studied.

2 Experimental

2.1 Chemicals

PTFE (60%) was purchased from Zhanyang Polymer Materials Co. Ltd., (Dongguan, China), potassium titanium oxalate ($K_2TiO(C_2O_4)\cdot 2H_2O$) was obtained from Mclean Biochemical Technology Co. Ltd. All other chemicals, such as ethanol (EtOH), Na_2SO_4, H_2SO_4, NaOH were all supplied by Sinopharm Co. Ltd., China. All the used chemicals were of analytical grade and did not need further purification.

2.2 Fabrication of Graphite/PTFE composite coating cathode

A 16-mesh 304 stainless-steel wire mesh was used as a current collector. The mesh was cut into strips of the same size and subjected to alkaline washing, acid pickling and water washing in sequence for removing surface impurities. For the preparation of composite coating, required amounts of graphite powder and anhydrous ethanol were mixed with ultrasonic stirring for 10 min, then PTFE emulsion with a mass ratio of graphite to PTFE of 3:1 was added to the mixture. After another 25 min of ultrasonic treatment, the highly dispersed mixture was stirred at about 70 ℃ to get a wet paste. An appropriate amount of graphite/PTFE wet paste was uniformly coated on both sides of the pretreated stainless steel mesh to form cathodes with varying thickness (0.75, 1.10, and 1.50 mm) and surface area (8, 12, and 16 cm^2). Then the cathodes were dried at 80 ℃ for 20 min, and eventually annealed at 350 ℃ for 60 min.

2.3 Electrogeneration of H_2O_2

The H_2O_2 electrogeneration experiments were performed at room temperature in an undivided plexiglass reactor containing 250 mL of 0.05 M Na_2SO_4 electrolyte, controlled by a direct current regulated power supply under constant current mode. The fabricated composite coating electrodes and Ti/RuO_2-IrO_2

(5×10 cm^2) acted as cathode and anode, respectively. The cathode and anode were vertically placed in parallel in the middle of the electrolytic reactor, 2 cm from each other. The initial pH ranging from 3.0–11.0 was adjusted using 0.1 M H_2SO_4 or 0.1 M NaOH before electrolysis. Oxygen (O_2) was bubbled into the solution near the cathode at a flow rate of 0.4 L·min^{-1}. At certain time intervals, the sample of 1.0 mL was taken out to determine the concentration of H_2O_2 quantitatively.

2.4 Characterization and analytical methods

The scanning electron microscopy (SEM) morphologies of graphite/PTFE coating cathodes were characterized on a Hitachi SU8010 microscope operated at 5.0 kV. Measurements of contact angles between distilled water and the fabricated electrodes were carried out by a contact angle meter (JC2000X, China).

H_2O_2 concentration was measured on a UV-visible spectrophotometer (UV–3300, MAPADA) with a potassium titanium (IV) oxalate method (Sellers et al. 1980).

2.5 Electrochemical Measurements

The cyclic voltammetry (CV) curves of the graphite/PTFE coating cathodes with different thicknesses were investigated by a CHI660E electrochemical station at a scan rate of 100 mV·s^{-1}. Electrochemical impedance spectroscopy (EIS) analyses were observed at frequencies from 10 kHz to 0.01 Hz with an amplitude of 5 mV. Graphite/PTFE coating cathode, platinum plate, and saturated calomel electrode (SCE) were used as working electrode, counter electrode and reference electrode, respectively. O_2-saturated 0.05 M Na_2SO_4 solution (pH 3.0) was prepared as the electrolyte.

2.6 Calculation of the Current Efficiency and Energy Consumption

The experimental current efficiency (CE) for H_2O_2 production was calculated from Eq. 5.

$$CE=\frac{nFCV}{\int_0^t I\mathrm{d}t}\times 100\% \quad (5)$$

Where n is the number of electrons transferred from oxygen to H_2O_2, (n=2), F is the Faraday constant (96486 C·mol^{-1}), C is the concentration of H_2O_2 (mol·L^{-1}), V is the volume of electrolyte (L), I is the applied current (A), and t is the electrolysis time (s).

The experimental energy consumption (EC, kWh•kg^{-1}) of generating 1 kg H_2O_2 was calculated according to Eq. 6.

$$EC=\frac{UIt}{3600CMV} \quad (6)$$

Where U is the electrolytic reactor voltage (V), M is the molar mass of H_2O_2 (34.01 g·mol^{-1}).

3 Results And Discussion

3.1 Cyclic Voltammetry (CV)

To determine the effect of cathode thickness on oxygen reduction reactivity, cyclic voltammetry experiments were carried out in 0.05 M Na_2SO_4 aqueous solution at pH 3.0. As seen in Fig. 1, no apparent reduction current peak was found in the CV curves of 1.50 mm cathode, while two reduction peaks occurred both in the CV curves of 0.75 mm and 1.10 mm cathode, which were inferred to correspond to the 2 e^- and 4 e^- ORRs (El-Deab et al. 2006; Gokdogan et al. 2006). The first reduction peak of the 0.75 mm cathode was identified at 0.351 V versus SCE, which was 11 mV more positive than that of 1.10 mm cathode. Meanwhile, a thin cathode exhibited a higher current response than a thick one. The obvious current peak indicated that more oxygen underwent a electrochemical transition from O_2 to H_2O_2, which was probably attributed to the improvement of O_2 and H_2O_2 mass transfer in a thinner graphite/PTFE composite cathode.

3.2 Electrochemical impedance spectroscopy (EIS)

The Nyquist plot in Fig. 2 shows the EIS results of cathodes with different thicknesses. As revealed in Fig. 2, the 0.75 mm cathode possessed the smallest arc radius compared with other cathodes, signifying lower charge transfer resistance and enhanced interfacial charge transfer efficiency. A thick cathode formed by excessive graphite/PTFE paste could block the transmission channels of the ions and O_2 (Ren et al. 2016), resulting in a large electron-transfer resistance and low electrochemical efficiency.

3.3 Influence of cathode thickness on H_2O_2 production and CE

Through constant current electrolysis, influence of cathode thickness on the H_2O_2 electrosynthesis was investigated. As presented in Fig. 3a, the H_2O_2 concentrations using the cathodes with different thicknesses of 0.75, 1.10, and 1.50 mm were 207.5, 172.3, and 143.7 $mg{\cdot}L^{-1}$, respectively. The corresponding CE values were calculated to be 34.1%, 28.3%, and 23.6% (Fig. 3b). These results demonstrated that the cathode thickness had a significant influence on the production of H_2O_2 and CE. The decrease of H_2O_2 production and CE was likely attributed to the increase of oxygen diffusion distance and electron-transfer resistance as the cathode thickness increased.

3.4 Influence of cathode area on H_2O_2 production and CE

Influence of cathode area on H_2O_2 electrogeneration was investigated using three fabricated graphite/PTFE coating cathodes. The surface areas of the coating cathodes were selected as 8, 12, and 16 cm^2 with the same cathode thickness of 0.75 mm. It can be seen from Fig. 4a and 4b that increasing the cathode geometric area was a convenient way to enhance H_2O_2 production and CE. After 180 minutes of reaction, the H_2O_2 generation using the cathode of 16 cm^2 was 72.1% and 222.2% higher than that of

the 12 cm^2 and 8 cm^2 cathodes, respectively, and the CE of the 16 cm^2 cathode was always higher than the other two cathodes. This enhancement was strongly correlated to the increase of effective surface areas of the graphite/PTFE coating cathode. Large surface can expand the three-phase contact area of O_2, cathode and electrolyte, thus more O_2 was absorbed at the cathode surface and electrochemically reduced to H_2O_2 via the 2 e^- pathway.

3.5 Influence of initial pH on H_2O_2 production and CE

As shown in Fig. 5a and 5b, the H_2O_2 accumulation and CE under acidic condition (pH 3.0) were both apparently higher than that in neutral and alkaline conditions. The H_2O_2 yield and CE decreased with the rising pH, whereby the H_2O_2 concentration and CE reached the lowest values 41.7 $mg{\cdot}L^{-1}$ and 6.8%, respectively, at electrolyte pH 11.0. This trend can be interpreted from Eq. (3) that H^+ was one of the reactants for the electrosynthesis of H_2O_2, and therefore, the relatively high acidity may play a beneficial effect on the enhancement of the reaction. In the pH range of 7.0–11.0, the H^+ concentration was insufficient for the 2 e^- ORR, what is worse, H_2O_2 principally exists as HO_2^- in strong alkaline solutions that can effectively catalyze the decomposition of H_2O_2 (Eq. 7 and 8) (Qiang et al. 2002). Thus, it is understandable that the H_2O_2 production and CE were the lowest in the electrolyte of pH 11.0.

$$O_2 + H_2O + 2e^- \rightarrow HO_2^- + OH^- \quad (7)$$

$$H_2O_2 + HO_2^- \rightarrow H_2O + O_2 + OH^- \quad (8)$$

3.6 Influence of current density on H_2O_2 production and CE

Figure 6a shows that the cumulative H_2O_2 concentration at 180 min enhanced gradually from 207.5 to 559.1 $mg{\cdot}L^{-1}$ with the increase of applied current density from 5 to 30 $mA{\cdot}cm^{-2}$, showing that the graphite/PTFE coating cathodes exhibited high activity in the investigated current density range. A higher current density could supply more electrons, speeding up the 2 e^- reduction of O_2 to H_2O_2. Meanwhile, 4 e^- reduction with H_2O generation (Eq. 4), H^+ reduction reaction with H_2 generation (Eq. 9) and other side reactions were more likely to occur simultaneously, which were in competition with the 2 e^- ORR. Therefore, the gradual decrease in CE from 34.1–15.3% (Fig. 6b) and severe increase in corresponding EC (Fig. 7) from 12.0 to 68.7 $kWh{\cdot}kg^{-1}$ at 180 min electrolysis with the increase of current density can be well explicated.

$$2H^+ + 2e^- \rightarrow H_2 \quad (9)$$

3.7 Cathode durability

Durability study of the graphite/PTFE coating cathode was investigated under the working conditions of current density 5 $mA{\cdot}cm^{-2}$, in an oxygen-saturated pH 3 solution. The H_2O_2 production was measured

and electrolyte was replaced with fresh one every 180 min. As presented in Fig. 8, the H_2O_2 production decreased gradually from 207.5 to 150.1 mg·L^{-1}, while the CE showed a decreasing tendency as well, going down from 34.0–24.3% after 5 recycles. The reason was attributed to the degradation of graphite/PTFE coating cathode performance with time. When the cathode was immersed in the electrolyte and catalyzed for a long time, excess water and cations would enter the electrode, that could block the pores of the cathode, thus reducing oxygen accessibility to the active site (Bidault et al.2009). In addition, the corrosion damage caused by the oxidation of graphite/PTFE would coating also reduce the H_2O_2 production performance of the cathode performance. The SEM images (Fig. 9a and 9b) distinctly confirmed the changes in the cathode surface morphology before and after the durability test. After 5 cycles, some graphite flakes peeled off from the cathode surface, causing cracks and a decrease in surface hydrophobicity. Contact angle measurement results (Fig. 9b and 9c) confirmed that the contact angle between cathode and solution diminished from 130.0° to 127.5° after 5 recycles. To achieve better restoration and regeneration performance, attention can be focused on various functionalization methods such as loading hydrophobic organic groups and coating exterior hydrophobic films on the electrode surface.

4 Conclusions

The thickness and surface area of graphite/PTFE coating cathodes were critical in electrogeneration of H_2O_2. Thin cathode design could reduce the interfacial charge transfer resistance, facilitate O_2 diffusion and transmission, and thus was conducive to the activity and selectivity of H_2O_2 production via 2 e^- ORR. At the same time, a large cathode area exposed more ORR sites, increased the contact area between cathode and O_2, thus enhancing H_2O_2 electrogeneration. The cathode with an active area of 16 cm^2 and a thickness of 0.75 mm achieved the highest H_2O_2 accumulation and CE among the investigated electrodes. The initial electrolyte pH appreciably impacted the H_2O_2 production in the range of 3.0–11.0. The graphite/PTFE coating cathode possessed the highest H_2O_2 generation rate and CE at pH 3.0, that was due to higher 2 e^- ORR activity under acidic conditions. Under alkaline conditions, the H_2O_2 production decreased significantly, probably because the generated HO_2^- promoted the decomposition of H_2O_2. Additionally, increasing current density from 5 to 30 mA·cm^{-2} prominently promoted H_2O_2 electrogeneration from 207.5 to 559.1 mg·L^{-1}, accompanying an opposite tendency in CE from 34.1–15.3% at 180 min. After the graphite/PTFE coating cathode was reused, the coating would be damaged and hydrophobicity would be reduced, resulting in the gradual decline of H_2O_2 production performance.

Declarations

Acknowledgement

This research is supported by the National Natural Science Foundation of China (51308284), the Postgraduate Research & Practice Innovation Program ofJiangsu Province(SJCX21_0461).

Funding

This research is financially supported by the National Natural Science Foundation of China (51308284), the Postgraduate Research & Practice Innovation Program ofJiangsu Province(SJCX21_0461).

Conflict of interest

The authors declare no conflict of interest.

Ethics approval

Not applicable.

Consent to participate

Not applicable.

Consent for publication

Not applicable.

Data availability statement

All data included in this study are available upon request by contact with the corresponding author.

References

1. HageR,LienkeA(2006)Applications of transition-metal catalysts to textile and wood-pulp bleaching. AngewChemIntEd45(2):206–222. http://doi.org/10.1002/anie.200500525
2. ZhangJ, ZhangH, ChengMJ, Lu, Q(2020)Tailoring the Electrochemical Production of H_2O_2: Strategies for the Rational Design of High-Performance Electrocatalysts. Small 16(15):1902845. http://doi.org/10.1002/smll.201902845
3. KimJH, KimYT, JooSH(2020)Electrocatalyst design for promoting two-electron oxygen reduction reaction: Isolation of active site atoms. Curr Opin Electroche 21:109–116. http://doi.org/10.1016/j.coelec.2020.01.007
4. LiuZ, Wardenier N, HosseinzadehS et al (2018)Degradation of bisphenol A by combining ozone with UV and H_2O_2 in aqueous solutions: mechanism and optimization.Clean Technol Envir20(9):2109–2118. http://doi.org/10.1007/s10098-018-1595-2
5. YangS, Verdaguer-CasadevallA, ArnarsonL et al (2018)Toward the Decentralized Electrochemical Production of H_2O_2: A Focus on the Catalysis. ACS Catal8(5):4064–4081. http://doi.org/10.1021/acscatal.8b00217
6. Seh ZW, KibsgaardJ, DickensCF, ChorkendorffIB, NorskovJK, JaramilloTF(2017)Combining theory and experiment in electrocatalysis: Insights into materials design. Science355(6321):eaad4998. http://doi.org/10.1126/science.aad4998

7. MelchionnaM, FornasieroP, PratoM(2019)The Rise of Hydrogen Peroxide as the Main Product by Metal-Free Catalysis in Oxygen Reductions. AdvMater31(13):1802920. http://doi.org/10.1002/adma.201802920
8. KimHW, RossMB, Kornienko N, Zhang L, Guo J, Yang P, McCloskeyBD(2018)Efficient hydrogen peroxide generation using reduced graphene oxide-based oxygen reduction electrocatalysts. Nat Catal1(4):282–290. http://doi.org/10.1038/s41929-018-0044-2
9. XiaC, XiaY, ZhuP, FanL, WangHT(2019)Direct electrosynthesis of pure aqueous H_2O_2 solutions up to 20% by weight using a solid electrolyte. Science366(6462):226–231. http://doi.org/10.1126/science.aay1844
10. Li H, Wen P, Itanze DS et al (2020) Scalable neutral H_2O_2 electrosynthesis by platinum diphosphide nanocrystals by regulating oxygen reduction reaction pathways. Nat Commun 11(1):3928. http://doi.org/10.1038/s41467-020-17584-9
11. AlJaberiFY(2019)Operating cost analysis of a concentric aluminum tubes electrodes electrocoagulation reactor. Heliyon5(8):e02307–e02307. http://doi.org/10.1016/j.heliyon.2019.e02307
12. WangZ, JamesDK, TourJM(2021)Metal-Free Electrocatalysts for Oxygen Reduction to Hydrogen Peroxide. Adv EnergySustainability Res2(7):2100021. http://doi.org/10.1002/aesr.202100021
13. Jiang Y, Ni P, Chen C et al (2018) Selective Electrochemical H_2O_2 Production through Two-Electron Oxygen Electrochemistry. Adv Energy Mater 8(31):1801909. http://doi.org/10.1002/aenm.201801909
14. SiahrostamiS, Verdaguer-CasadevallA, KaramadM et al(2013)Enabling direct H_2O_2 production through rational electrocatalyst design. Nat Mater 12(12):1137–1143. http://doi.org/10.1038/nmat3795
15. Moreira J, Lima VB, Goulart LA, Lanza MRV (2019) Electrosynthesis of hydrogen peroxide using modified gas diffusion electrodes (MGDE) for environmental applications: Quinones and azo compounds employed as redox modifiers. Appl Catal B-Environ 248:95–107. http://doi.org/10.1016/j.apcatb.2019.01.071
16. Pham-Truong TN, Petenzi T, Ranjan C, Randriamahazaka H, Ghilane J (2018) Microwave assisted synthesis of carbon dots in ionic liquid as metal free catalyst for highly selective production of hydrogen peroxide. Carbon 130:544–552. http://doi.org/10.1016/j.carbon.2018.01.070
17. Da PozzoA, Di Palma L, Merli C, PetrucciE(2005)An experimental comparison of a graphite electrode and a gas diffusion electrode for the cathodic production of hydrogen peroxide.J Appl Electrochem 35(4):413–419. http://doi.org/10.1007/s10800-005-0800-2
18. WangY, LiuY, WangK, Song S, TsiakarasP, Liu H(2015)Preparation and characterization of a novel KOH activated graphite felt cathode for the electro-Fenton process. Appl Catal B-Environ 165:360–368. http://doi.org/10.1016/j.apcatb.2014.09.074

19. Zhao Y, Cui J, Zhou W, Hojabri S, Alshawabkeh AN (2020) Electrogeneration of H_2O_2 utilizing anodic O_2 on polytetrafluoroethylene-modified cathode in flow-through reactor. Electrochem commun 121:106868. http://doi.org/10.1016/j.elecom.2020.106868
20. ZhouW, RajicL, ZhaoY, GaoJ, QinY, AlshawabkehAN(2018)Rates of H_2O_2 Electrogeneration by Reduction of Anodic O_2 at RVC Foam Cathodes in Batch and Flow-through Cells. Electrochim Acta277:185–196. http://doi.org/10.1016/j.electacta.2018.04.174
21. PérezJF, Sabatino S, Galia A, RodrigoMA, Llanos J, SáezC, Scialdone O(2018)Effect of air pressure on the electro-Fenton process at carbon felt electrodes. Electrochim Acta273:447–453. http://doi.org/10.1016/j.electacta.2018.04.031
22. Ma P, Ma H, Galia A, Sabatino S, Scialdone O (2019) Reduction of oxygen to H_2O_2 at carbon felt cathode in undivided cells. Effect of the ratio between the anode and the cathode surfaces and of other operative parameters. Sep. Purif. Technol 208:116–122. http://doi.org/10.1016/j.seppur.2018.04.062
23. Wang AM, QuJH, RuJ, Liu HJ, GeJT(2005)Mineralization of an azo dye Acid Red 14 by electro-Fenton's reagent using an activated carbon fiber cathode. Dyes Pigments65(3):227–233. http://doi.org/10.1016/j.dyepig.2004.07.019
24. Xia G, Lu Y, Xu H (2015) Electrogeneration of hydrogen peroxide for electro-Fenton via oxygen reduction using polyacrylonitrile-based carbon fiber brush cathode. Electrochim Acta 158:390–396. http://doi.org/10.1016/j.electacta.2015.01.102
25. Zarei M, Salari D, Niaei A, Khataee A (2009)Peroxi-coagulation degradation of CI Basic Yellow 2 based on carbon-PTFE and carbon nanotube-PTFE electrodes as cathode. Electrochim Acta 54(26):6651–6660. http://doi.org/10.1016/j.electacta.2009.06.060
26. Park J, Nabae Y, Hayakawa T, Kakimoto MA (2014) Highly Selective Two-Electron Oxygen Reduction Catalyzed by Mesoporous Nitrogen-Doped Carbon. ACS Catal 4(10):3749–3754. http://doi.org/10.1021/cs5008206
27. Thostenson JO, Ngaboyamahina E, Sellgren KL et al (2017) Enhanced H_2O_2 Production at Reductive Potentials from Oxidized Boron-Doped Ultrananocrystalline Diamond Electrodes. ACS Appl Mater Interfaces9(19):16610–16619. http://doi.org/10.1021/acsami.7b01614
28. Shiraishi Y, Kofuji Y, Sakamoto H, Tanaka S, Ichikawa S, Hirai T (2015) Effects of Surface Defects on Photocatalytic H_2O_2 Production by Mesoporous Graphitic Carbon Nitride under Visible Light Irradiation. ACS Catal 5(5):3058–3066. http://doi.org/10.1021/acscatal.5b00408
29. Liu Y, Quan X, Fan X, Wang H, Chen S (2015) High-Yield Electrosynthesis of Hydrogen Peroxide from Oxygen Reduction by Hierarchically Porous Carbon. Angew Chem Int Edit 54(23):6837–6841. http://doi.org/10.1002/anie.201502396
30. Zhou L, Hu Z, Zhang C, Bi Z, Jin T,Zhou M(2013) Electrogeneration of hydrogen peroxide for electro-Fenton system by oxygen reduction using chemically modified graphite felt cathode. Sep. Purif. Technol 111:131–136. http://doi.org/10.1016/j.seppur.2013.03.038

31. Oliaii E, Desilets M, Lantagne G (2018) Effect of the design parameters on mass transfer and energy consumption inside a lithium electrolysis cell. J Appl Electrochem 48(6):725–737. http://doi.org/10.1007/s10800-018-1179-1
32. Sellers RM(1980) Spectrophotometric determination of hydrogen peroxide using potassium titanium (IV) oxalate. Analyst105(1255):950–954. http://doi.org/10.1039/an9800500950
33. El-Deab MS, Sotomura T, Ohsaka T (2006) Oxygen reduction at Au nanoparticles electrodeposited on different carbon substrates. Electrochim Acta52(4):1792–1798. http://doi.org/10.1016/j.electacta.2005.12.057
34. Gokdogan O, Sulak M, Gulce H (2006) Investigation of oxygen electroreduction on polyvinylferrocene coated glassy carbon electrodes. Chem. Eng. J 116(1):39–45. http://doi.org/10.1016/j.cej.2005.10.016
35. Ren W, Tang D, Lu X, Sun J, Li M, Qu S, Fan D(2016) Novel Multilayer ACF@rGO@OMC Cathode Composite with Enhanced Activity for Electro-Fenton Degradation of Phthalic Acid Esters. Ind Eng Chem Res 55(42):11085–11096. http://doi.org/10.1021/acs.iecr.6b02896
36. Qiang ZM, Chang JH, Huang CP (2002) Electrochemical generation of hydrogen peroxide from dissolved oxygen in acidic solutions. Water Res 36(1):85–94. http://doi.org/10.1016/s0043-1354(01)00235-4
37. Bidault F, Brett DJL, MiddletonPH, BrandonNP (2009) Review of gas diffusion cathodes for alkaline fuel cells. JPower Sources187:39–48. http://doi.org/10.1016/j.jpowsour.2008.10.106

Figures

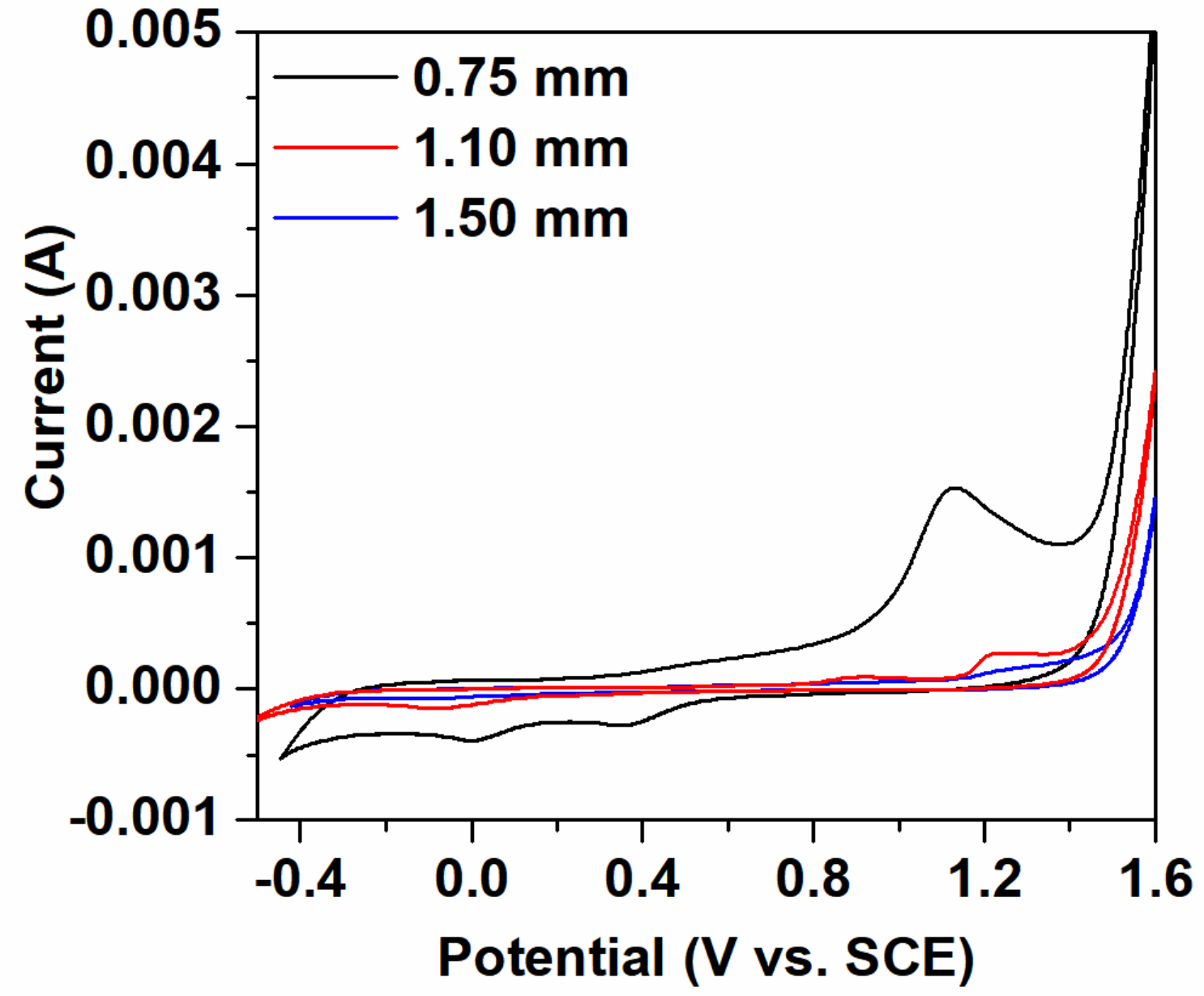

Figure 1

The cyclic voltammetry of cathodes with different thicknesses

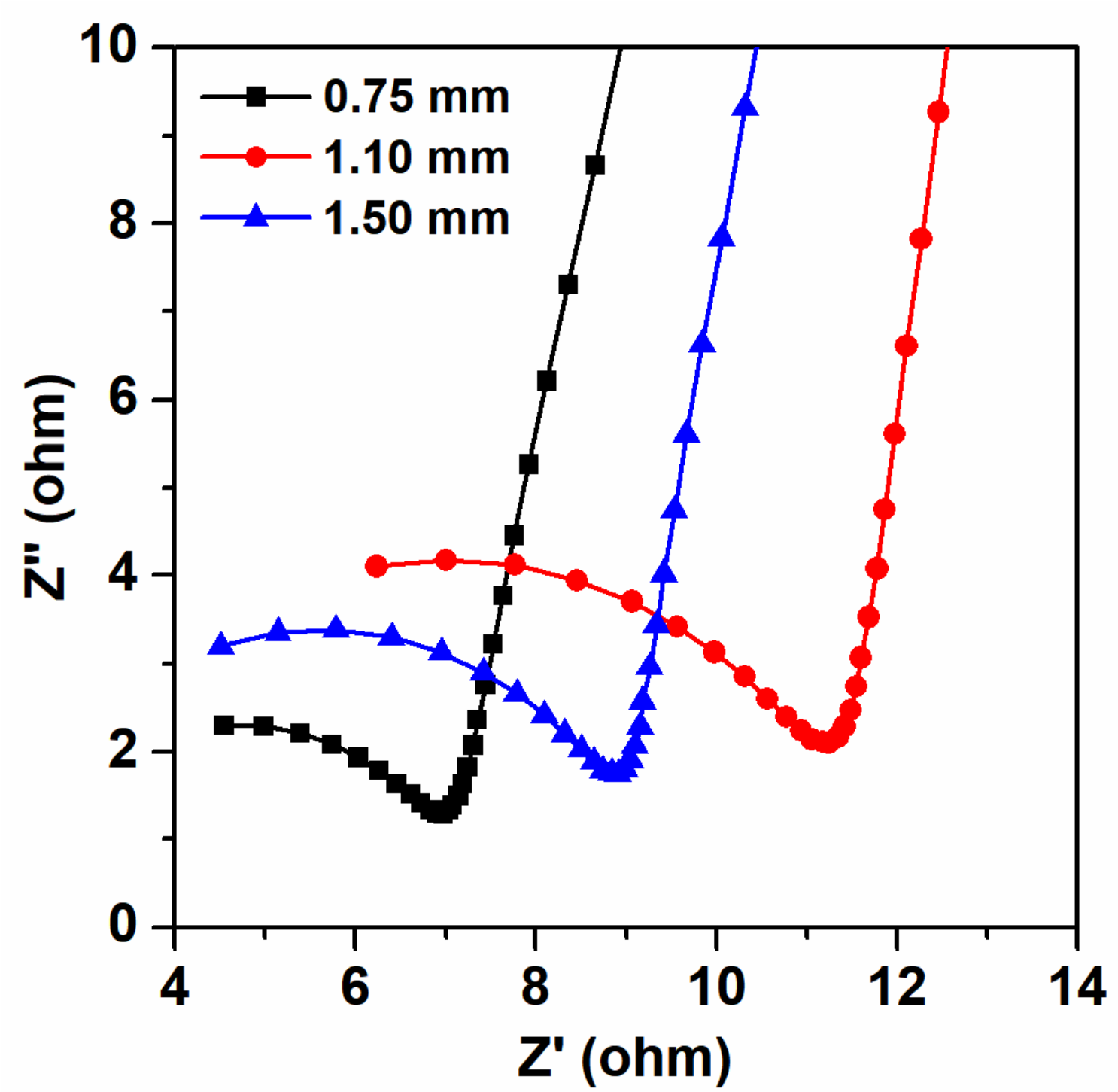

Figure 2

Nyquist plots of the cathodes with different thicknesses

Figure 3

Influence of cathode thickness on H_2O_2 production (a) and CE (b). Conditions: pH 3.0, current density 5 $mA{\cdot}cm^{-2}$, 0.05 $mol{\cdot}L^{-1}$ Na_2SO_4, Q_{oxygen} = 0.4 $L{\cdot}min^{-1}$

Figure 4

Influence of cathode area on H_2O_2production (a) and CE (b). Conditions: pH 3.0, current density 5 $mA{\cdot}cm^{-2}$, 0.05 $mol{\cdot}L^{-1}$ Na_2SO_4,Q_{oxygen} = 0.4 $L{\cdot}min^{-1}$

Figure 5

Influence of pH on H_2O_2 production (a) and CE (b). Conditions: current density 5 $mA{\cdot}cm^{-2}$, 0.05 $mol{\cdot}L^{-1}$ Na_2SO_4, Q_{oxygen} = 0.4 $L{\cdot}min^{-1}$

Figure 6

Influence of current density on H_2O_2 production (a) and CE (b). Conditions: pH 3.0, 0.05 $mol{\cdot}L^{-1}$ Na_2SO_4, Q_{oxygen} = 0.4 $L{\cdot}min^{-1}$

Figure 7

Influence of current density on energy consumption

Figure 8

Recycle experiments for electrogeneration of H_2O_2 using graphite/PTFE coating cathode.

Conditions: pH 3.0, current density 5 $mA{\cdot}cm^{-2}$, 0.05 $mol{\cdot}L^{-1}$ Na_2SO_4, Q_{oxygen} = 0.4 $L{\cdot}min^{-1}$

Figure 9

SEM images(a, b)and surface contact angle results (c, d)of the cathodes before and after the durability test

Supplementary Files

This is a list of supplementary files associated with this preprint. Click to download.

- GraphicalAbstract.png